

## Solid-state MAS NMR Investigation on the Local Structures of $xV_2O_5-B_2O_3-yNa_2O$ Glasses

Sun Ha Kim, Oc Hee Han,<sup>†</sup> Jae Pil Kang,<sup>‡</sup> and Seung Ki Song<sup>†</sup>

Daegu Center, Korea Basic Science Institute, Daegu 702-701, Korea. \*E-mail: ohhan@kbsi.re.kr

<sup>†</sup>Department of Physics, Myongji University, Yongin 449-728, Korea

Received November 18, 2008, Accepted January 16, 2009

The local structures of the boron and vanadium sites in the ternary glass  $xV_2O_5-B_2O_3-yNa_2O$  were studied by  $^{11}B$  and  $^{51}V$  magic angle spinning (MAS) nuclear magnetic resonance (NMR). With increasing  $x$ , the mole ratios of the  $BO_3$  and  $BO_4$  structures were enhanced, as were the quadrupole asymmetry parameters for the  $BO_3$  structures, while the quadrupole coupling constants for the sites were reduced. However, the opposite trends were observed with increasing  $y$ , implying that  $V_2O_5$  and  $Na_2O$  play opposite roles. The  $VO_4$ ,  $VO_5$  and  $VO_6$  structures with all oxygens bonded to the vanadium neighbors were identified. Vanadiums bonded to the greater number of oxygens were more populated at higher contents of  $Na_2O$  and  $V_2O_5$ . In addition, the  $VO_4$  structures with at least one oxygen bonded to boron instead of vanadium were detected at low  $Na_2O$  contents. The electron densities of various vanadium oxide structures were affected by the weight densities and vanadium ion densities. The  $VO_4$  structures were more likely to be vanadium oxide structures right next to  $V^{4+}$  ions.

**Key Words:** Glass structure, Nuclear magnetic resonance, MAS NMR

### Introduction

Although glasses based on  $V_2O_5$  were successfully prepared in the mid 1800s, the semiconducting property of the glasses was reported by Denton *et al.* almost a century later in 1954.<sup>1</sup> Since the conductivity of various vanadate glasses was reported to be due to electrons rather than ionic diffusion,<sup>2</sup> various vanadate glasses have attracted research attention, especially on their conducting properties.<sup>3,4</sup>  $V_2O_5$  does not form a good glass by itself but does form homogeneous glasses with  $B_2O_3$ .<sup>1,5</sup> The addition of a small amount of glass network forming oxide to these boro-vanadate glasses was reported to simplify the glass formation.<sup>6</sup> One of the procedures to optimize the properties of mixed glasses has been to change the glass compositions.<sup>1-8</sup> However, the relationships between the local structures and the glass properties have not yet been fully elucidated.

Solid-state nuclear magnetic resonance (NMR) is an excellent

spectroscopic methodology to probe the local structures of inorganic materials, especially glasses, since it does not require a sample to have long-range order. Since boron bonded to 3 and 4 oxygens ( $BO_3$  and  $BO_4$  structures, respectively) in alkali borate glasses was identified by  $^{11}B$  NMR by Bray *et al.*,<sup>8</sup> binary and ternary borate glasses have been studied extensively by  $^{11}B$  NMR and corresponding structural models of the glasses have been reported.<sup>9,10</sup> Likewise,  $^{51}V$  NMR studies on various vanadate glasses have been carried out.<sup>6,11-15</sup> In this work, we identify the local structures of  $xV_2O_5-B_2O_3-yNa_2O$  glasses for various levels of  $x$  and  $y$  using  $^{11}B$  and  $^{51}V$  magic angle spinning (MAS) NMR where  $x$  is the mole ratio of  $V_2O_5$  to  $B_2O_3$  and  $y$  is the mole ratio of  $Na_2O$  to  $B_2O_3$ .

### Experimental

**Sample preparation.** Samples were prepared as described in detail in reference.<sup>16</sup> Ternary  $xV_2O_5-B_2O_3-yNa_2O$  glasses.

**Table 1.**  $^{11}B$  MAS NMR spectra simulation results of the  $xV_2O_5-B_2O_3-yNa_2O$  glasses

| $y$          | Relative population of $BO_3$ structure (%) | Relative population of $BO_4$ structure (%) | Qcc of $BO_3$ structure (MHz) | $\eta$ of $BO_3$ structure |             |
|--------------|---|---|-------------------------------|----------------------------|-------------|
| at $x = 2.5$ | 0.25  | 87 ± 1                                      | 13 ± 1                        | 2.50 ± 0.01                | 0.28 ± 0.01 |
|              | 0.5   | 83 ± 1                                      | 17 ± 1                        | 2.52 ± 0.01                | 0.26 ± 0.01 |
|              | 1.0   | 79 ± 1                                      | 21 ± 1                        | 2.53 ± 0.01                | 0.25 ± 0.01 |
|              | 1.5   | 62 ± 1                                      | 38 ± 2                        | 2.55 ± 0.01                | 0.24 ± 0.01 |
|              | 2.0   | 61 ± 2                                      | 39 ± 2                        | 2.56 ± 0.01                | 0.21 ± 0.01 |
| $x$          | Relative population of $BO_3$ structure (%) | Relative population of $BO_4$ structure (%) | Qcc of $BO_3$ structure (MHz) | $\eta$ of $BO_3$ structure |             |
| at $y = 2.0$ | 1.0   | 47 ± 1                                      | 53 ± 1                        | 2.60 ± 0.01                | 0.13 ± 0.01 |
|              | 1.5   | 54 ± 1                                      | 46 ± 1                        | 2.59 ± 0.01                | 0.17 ± 0.01 |
|              | 2.0   | 63 ± 1                                      | 37 ± 1                        | 2.56 ± 0.01                | 0.19 ± 0.01 |
|              | 2.5   | 61 ± 1                                      | 39 ± 1                        | 2.56 ± 0.01                | 0.21 ± 0.01 |
|              | 3.0   | 62 ± 1                                      | 38 ± 1                        | 2.55 ± 0.01                | 0.23 ± 0.01 |

**Table 2.**  $^{51}V$  MAS NMR spectra simulation results of the  $xV_2O_5-B_2O_3-yNa_2O$  glasses

| y    | x    | Relative population (%)         |                 |                                 | FWHH (Hz)                       |                 |                 |                                 | Chemical shift (ppm)            |                 |                 |                                 |                 |
|------|------|---------------------------------|-----------------|---------------------------------|---------------------------------|-----------------|-----------------|---------------------------------|---------------------------------|-----------------|-----------------|---------------------------------|-----------------|
|      |      | with V-O-V bonding <sup>a</sup> |                 | with V-O-B bonding <sup>b</sup> | with V-O-V bonding <sup>a</sup> |                 |                 | with V-O-B bonding <sup>b</sup> | with V-O-V bonding <sup>a</sup> |                 |                 | with V-O-B bonding <sup>b</sup> |                 |
|      |      | VO <sub>4</sub>                 | VO <sub>5</sub> | VO <sub>6</sub>                 | VO <sub>4</sub>                 | VO <sub>5</sub> | VO <sub>6</sub> | VO <sub>4</sub>                 | VO <sub>5</sub>                 | VO <sub>6</sub> | VO <sub>4</sub> | VO <sub>5</sub>                 | VO <sub>6</sub> |
| 0.25 | 0.25 | -                               | -               | 100                             | -                               | -               | -               | 112                             | -                               | -               | -               | -                               | -641            |
|      | 0.5  | -                               | -               | 100                             | -                               | -               | -               | 113                             | -                               | -               | -               | -                               | -640            |
|      | 1.5  | 72                              | 5               | -                               | 23                              | 53              | 20              | -                               | 66                              | -592            | -619            | -                               | -655            |
|      | 2.0  | 60                              | 21              | -                               | 19                              | 58              | 18              | -                               | 55                              | -599            | -620            | -                               | -664            |
|      | 2.5  | 54                              | 32              | -                               | 14                              | 58              | 18              | -                               | 42                              | -615            | -620            | -                               | -674            |
|      | 3.0  | 47                              | 41              | -                               | 12                              | 58              | 18              | -                               | 38                              | -618            | -620            | -                               | -675            |
| 2.0  | 1.0  | 82                              | 18              | -                               | -                               | 46              | 58              | -                               | -                               | -564            | -587            | -                               | -               |
|      | 1.5  | 84                              | 16              | -                               | -                               | 46              | 66              | -                               | -                               | -581            | -605            | -                               | -               |
|      | 2.0  | 84                              | 12              | 4                               | -                               | 52              | 66              | 46                              | -                               | -584            | -617            | -536                            | -               |
|      | 2.5  | 71                              | 20              | 9                               | -                               | 58              | 76              | 48                              | -                               | -584            | -618            | -529                            | -               |
|      | 3.0  | 64                              | 24              | 14                              | -                               | 66              | 77              | 41                              | -                               | -584            | -622            | -520                            | -               |

The uncertainty is  $\pm 1$  for all the spectral simulation data in the table. <sup>a</sup>The VO<sub>4</sub>, VO<sub>5</sub> and VO<sub>6</sub> structures with all oxygens bonded to the vanadium neighbors <sup>b</sup>The VO<sub>4</sub> structures with at least one oxygen bonded to boron instead of vanadium

consisting of a glass network former of B<sub>2</sub>O<sub>3</sub>, a transition metal oxide of V<sub>2</sub>O<sub>5</sub>, and an alkaline metal oxide of Na<sub>2</sub>O. were produced first by weighing stoichiometric amounts of Na<sub>2</sub>CO<sub>3</sub>, H<sub>3</sub>BO<sub>3</sub>, and V<sub>2</sub>O<sub>5</sub> (all purchased from Aldrich, U.S.A.) and mixing them well. The mixture was dried in a vacuum oven at 150 °C for about 15 minutes and then transferred to a Pt crucible to melt in an electric furnace (Model 51333 of Lindberg Co., U.S.A.) at 1000 ~ 1100 °C for 30 minutes. A melted mixture was poured onto a smooth stainless steel sheet and covered with another stainless steel sheet to be quenched. Transparent dark brown glasses were produced and the glass quality was checked with an X-ray diffractometer (Model CN2013 of Rigaku, Japan). The nominal mixing mole ratios x and y of the  $xV_2O_5-B_2O_3-yNa_2O$  glasses were varied as indicated in Tables 1 and 2.

**Sample characterization.** The  $^{51}V$  and  $^{11}B$  MAS NMR spectra of the samples were acquired on a Bruker DSX 400 spectrometer with a Larmor frequency of 105.19 and 128.38 MHz, respectively. A spinning speed of 13 kHz with 4 mm zirconia rotors was employed for the  $^{11}B$  MAS NMR spectra while 30 kHz or higher spinning rates with 2.5 mm rotors were required to obtain resolved peaks in the  $^{51}V$  MAS NMR spectra. Pulse repetition delays of 20 s and 1  $\mu$ s excitation pulses (for a solution 90° pulse of 5  $\mu$ s) were used for the  $^{11}B$  MAS NMR spectra while pulse repetition delays of 1 s and 0.8  $\mu$ s excitation pulses (for a solution 90° pulse of 6.4  $\mu$ s) were used for the  $^{51}V$  MAS NMR spectra. All chemical shifts were referenced against neat VOCl<sub>3</sub> liquid, by using saturated NaVO<sub>3</sub> aqueous solution (-578 ppm), and against saturated H<sub>3</sub>BO<sub>3</sub> aqueous solution for the  $^{51}V$  and  $^{11}B$  spectra, respectively. All the NMR spectrum simulation was carried out with a WINFIT program (Bruker Biospin GmbH, Germany).

## Results and Discussion

**$^{11}B$  MAS NMR.** The  $^{11}B$  MAS NMR spectrum of the  $xV_2O_5-B_2O_3-yNa_2O$  glasses consisted of a center band with many spinning side bands. The center band exhibited a powder

pattern signal that was broadened by the second-order quadrupole interaction of planar triangle BO<sub>3</sub> structures, as well as a relatively sharp signal from tetrahedral BO<sub>4</sub> structures overlapped with the right shoulder of the powder pattern.<sup>10,16</sup> Figures 1 and 2 show the  $^{11}B$  MAS NMR spectra of the  $xV_2O_5-B_2O_3-yNa_2O$  glasses for various y ratios at x = 2.5 and for various x ratios at y = 2.0, respectively. The relative populations of the BO<sub>3</sub> and BO<sub>4</sub> structures, quadrupole parameters (quadrupole coupling constant, Qcc, and quadrupole asymmetry parameter,  $\eta$ ) of the BO<sub>3</sub> structures, summarized in Table 1, were obtained from the simulation of the center bands, as shown in the right columns in Figures 1 and 2. The relative populations of the BO<sub>3</sub> structures, as plotted

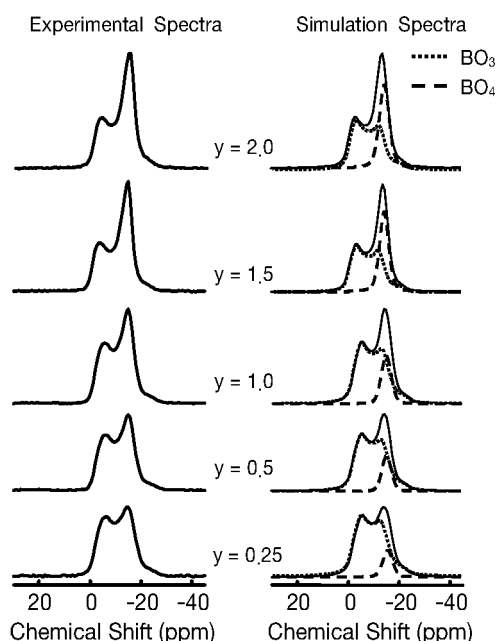


**Figure 1.** Experimental (left column) and simulated (right column)  $^{11}B$  MAS NMR spectra of the  $xV_2O_5-B_2O_3-yNa_2O$  glasses for various y at x = 2.5. The spectra were simulated with the signal contribution from the BO<sub>3</sub> and BO<sub>4</sub> structures.

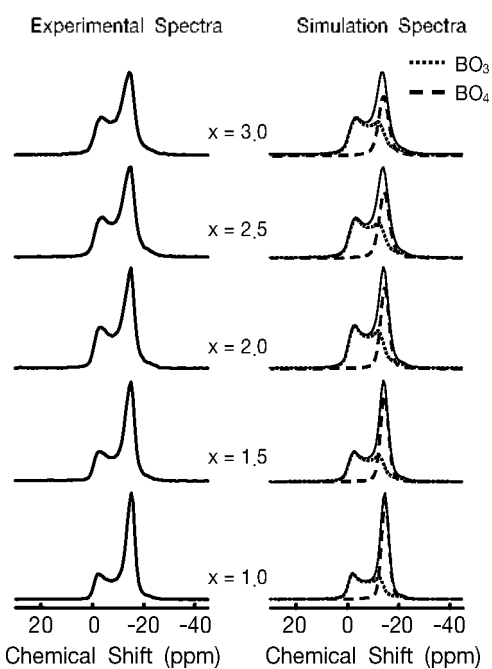


**Figure 2.** Experimental (left column) and simulated (right column)  $^{11}\text{B}$  MAS NMR spectra of the  $x\text{V}_2\text{O}_5\text{-B}_2\text{O}_3\text{-yNa}_2\text{O}$  glasses for various  $x$  at  $y = 2.0$ . The spectra were simulated with the signal contribution from the  $\text{BO}_3$  and  $\text{BO}_4$  structures.

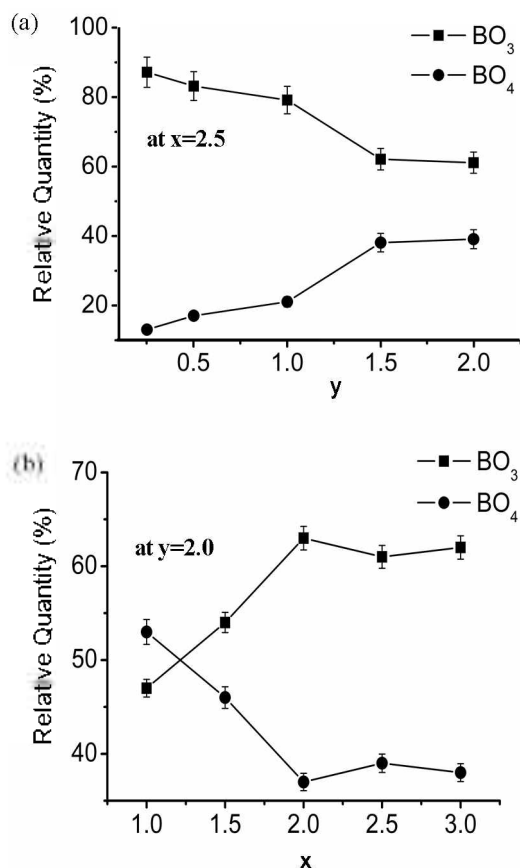


**Figure 3.** Relative population changes of the  $\text{BO}_3$  and  $\text{BO}_4$  structures in the  $x\text{V}_2\text{O}_5\text{-B}_2\text{O}_3\text{-yNa}_2\text{O}$  glasses for various  $y$  at  $x = 2.5$  (a) and for various  $x$  at  $y = 2.0$  (b).

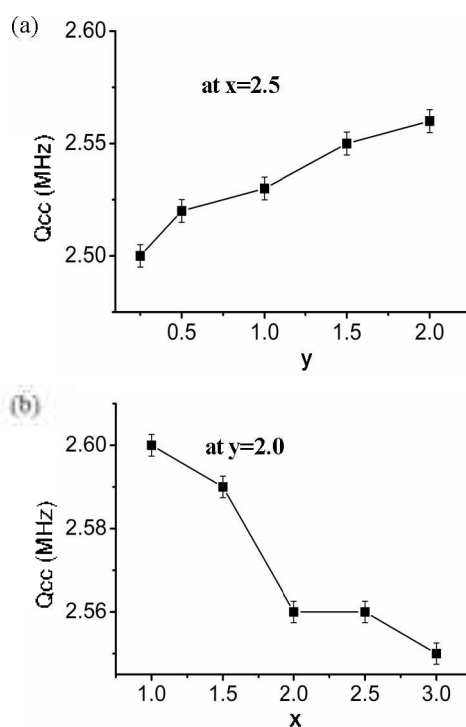


**Figure 4.** Quadrupole coupling constant ( $Q_{cc}$ ) changes of the  $\text{BO}_3$  structures in the  $x\text{V}_2\text{O}_5\text{-B}_2\text{O}_3\text{-yNa}_2\text{O}$  glasses for various  $y$  at  $x = 2.5$  (a) and various  $x$  at  $y = 2.0$  (b).

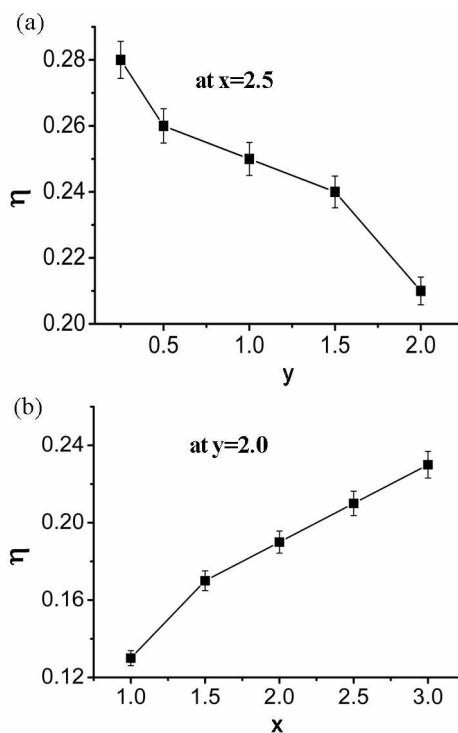


**Figure 5.** Quadrupole asymmetry parameter ( $\eta$ ) changes of the  $\text{BO}_3$  structures in the  $x\text{V}_2\text{O}_5\text{-B}_2\text{O}_3\text{-yNa}_2\text{O}$  glasses for various  $y$  at  $x = 2.5$  (a) and various  $x$  at  $y = 2.0$  (b).

in Figure 3, were reduced for increasing  $y$  up to 1.5 and then remained constant for larger  $y$  while they were increased for increasing  $x$  up to 2.0 and then remained constant for larger  $x$ .  $\text{Na}_2\text{O}$  apparently converted some of the  $\text{BO}_3$  structures into

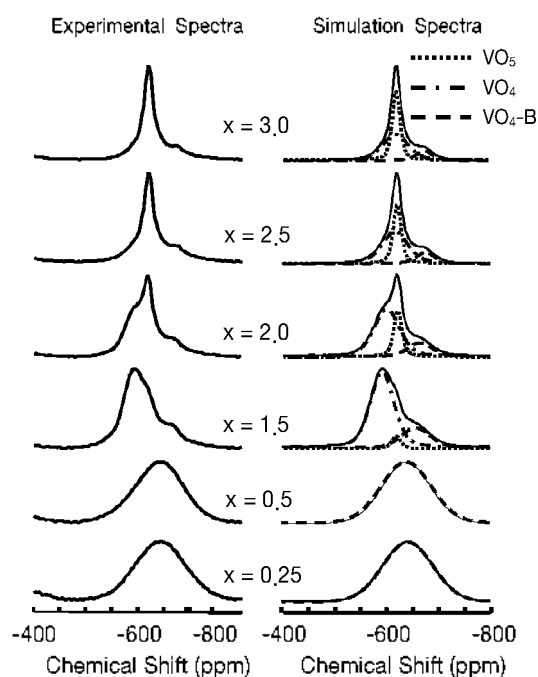


**Figure 6.** Experimental (left column) and simulated (right column)  $^{51}\text{V}$  MAS NMR spectra of the  $xV_2O_5-B_2O_3-yNa_2O$  glasses for various  $x$  at  $y = 0.25$ . The spectra were simulated with the peaks of the  $VO_4$  and  $VO_5$  structures with all oxygens bonded to the vanadium neighbors and of the  $VO_4$  structures with at least one oxygen bonded to boron instead of vanadium (denoted as  $VO_4\text{-B}$ ).

$BO_4$  structures by donating an oxygen atom to the  $BO_3$  structures and by existing as a  $Na^+$  ion in the glass up to  $y = 1.5$ , as reported previously.<sup>8,17</sup> With higher concentrations of  $Na_2O$  in the glass, the  $Na_2O$  did not seem to break up anymore. Likewise, the influence of  $V_2O_5$  on the relative populations of the  $BO_3$  and  $BO_4$  structures can be explained as follows:  $V_2O_5$  takes one oxygen atom from the  $BO_4$  structures at  $x$  up to 2.0, which thereby increases the relative population of the  $BO_3$  structures. The  $Q_{cc}$  value of the  $BO_3$  structures, plotted in Figure 4, increased with increasing  $y$  ratio but decreased with increasing  $x$  ratio. In contrast,  $\eta$  decreased with increasing  $y$  ratio but increased with increasing  $x$  ratio, as plotted in Figure 5. These quadrupole parameters indicated (1) that  $Na_2O$  increased the electric field gradients at the boron sites of the  $BO_3$  structures but reduced the distortion of the gradients and (2) that  $V_2O_5$  had the opposite effect on the electric field gradients.

**$^{51}\text{V}$  MAS NMR.** The  $^{51}\text{V}$  MAS NMR spectrum of the  $xV_2O_5-B_2O_3-yNa_2O$  glasses comprised center peaks for each V site and their corresponding spinning side bands. To remove the overlap of the spinning side bands with any center peaks, spinning rates higher than 29 kHz were required at 9.4 T. Four different center peaks, assigned to  $VO_6$ ,  $VO_5$ , and  $VO_4$  structures that were all bonded to neighboring vanadiums and to  $VO_4$  structure with at least one oxygen bonded to boron instead of vanadium,<sup>13,18,19</sup> were obtained from the spectral simulation of the spectra, as shown in Figures 6 and 7. The peaks at  $-587 \sim -622$  ppm were assigned to  $VO_5$  structures as in  $V_2O_5$ ,<sup>14,15,20</sup> those at  $-564 \sim -618$  ppm to  $VO_4$  structures,<sup>13,21,22</sup> those at  $-520 \sim -536$  ppm to  $VO_6$ ,<sup>21,22</sup> and those at

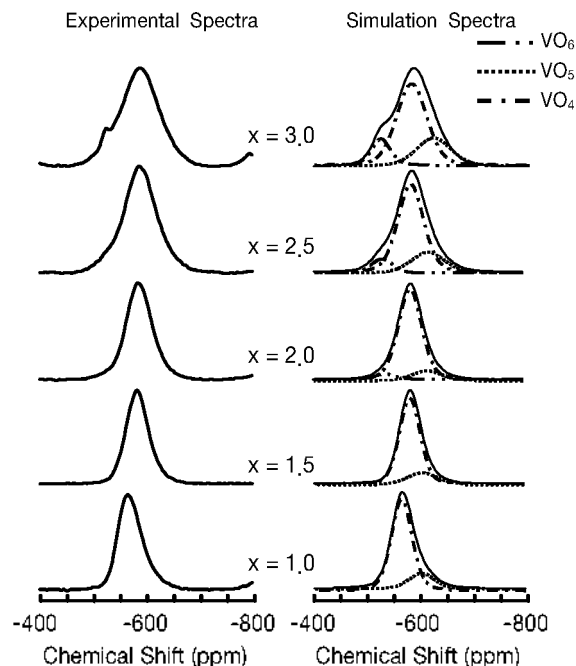


**Figure 7.** Experimental (left column) and simulated (right column)  $^{51}\text{V}$  MAS NMR spectra of the  $xV_2O_5-B_2O_3-yNa_2O$  glasses for various  $x$  at  $y = 2.0$ . The spectra were simulated with the peaks of the  $VO_4$ ,  $VO_5$ , and  $VO_6$  structures with all oxygens bonded to the vanadium neighbors.

$-640 \sim -675$  ppm to  $VO_4$  structures with at least one oxygen bonded to boron instead of vanadium.<sup>13</sup> The relative populations, peak widths, and chemical shifts of the different vanadium oxide structures are summarized in Table 2.

For the  $xV_2O_5-B_2O_3-yNa_2O$  glasses of  $y = 0.25$ , most of the vanadium sites were present as  $VO_4$  structures with at least one oxygen bonded to boron when  $y$  was less than or equal to 0.5, as shown in Figure 2 and Table 2. When  $x$  was greater than or equal to 1.5, the population of these  $VO_4$  structures was drastically reduced and  $VO_5$  and  $VO_4$  structures bonded to neighboring vanadiums were detected. At larger  $x$  ratios, the  $VO_5$  structures were formed in preference to the  $VO_4$  structures bonded to neighboring vanadiums. Therefore, in the  $xV_2O_5-B_2O_3-yNa_2O$  glasses of greater  $x$  ratio, the  $VO_5$  structures, i.e., the major structure in  $V_2O_5$ , were more produced in the glasses.

In contrast, the  $VO_4$  structures with at least one oxygen bonded to boron were not detected in the  $xV_2O_5-B_2O_3-yNa_2O$  glasses with  $y = 2.0$  even at small  $x$  ratios while the  $VO_6$  structures, which were not detected at all for  $y = 0.25$ , were observed at large  $x$  ratios. Thus, higher  $Na_2O$  content seemed to have promoted the formation of vanadium sites coordinated with more oxygens and to have simultaneously hindered V-O-B bonding formation. The full width at a half height (FWHM), a measure of the peak width, of the  $^{51}\text{V}$  spectra can be influenced by various factors such as the distributions of bond angles and lengths, kinds of the next nearest neighbor atoms, distances to paramagnetic centers such as  $V^{4+}$  ions, and quadrupole parameters at the vanadium sites. The Gaussian/Lorentzian peak shapes observed in our  $^{51}\text{V}$  spectra indicated that the quadrupolar line broadening is negligible in the center

peaks compared to the other line broadening factors. The vanadium nuclei too close to the paramagnetic centers would not be detected due to the strong dipole interaction with the unpaired electrons. Even when vanadium nuclei located a certain distance away from unpaired electrons are observed, the linewidths are widened in the  $^{51}\text{V}$  NMR spectra. If a random distribution and no-mutual-interaction of paramagnetic centers are assumed, the linewidths of all vanadium sites were expected to be influenced similarly. Therefore, the distances to paramagnetic centers such as  $\text{V}^{4+}$  were unlikely to have been the main cause of the linewidth variations for different vanadium sites observed in the  $^{51}\text{V}$  spectra as the glass compositions were varied. At  $y = 0.25$ , the most dramatic peak width changes were observed for the  $\text{VO}_4$  structures with at least one oxygen bonded to boron. The FWHH was narrowed as more  $\text{V}_2\text{O}_5$  components were present, as shown in Table 2, which was attributed to binding with fewer B and/or decreased local structural inhomogeneity with increasing  $\text{V}_2\text{O}_5$  components in the glass. On the other hand, the FWHH of the  $\text{VO}_5$  and  $\text{VO}_4$  structures became slightly wider at  $y = 2.0$  with increasing  $\text{V}_2\text{O}_5$  components, suggesting that the  $\text{VO}_5$  and  $\text{VO}_4$  structures had wider structural heterogeneities, in the presence of the high  $\text{Na}_2\text{O}$  concentration ( $y = 2.0$ ), with increasing  $\text{V}_2\text{O}_5$  concentration. The chemical shifts of the vanadium sites remained constant (for the  $\text{VO}_5$  structure at  $y = 0.25$ ), were downfield shifted (for the  $\text{VO}_6$  structure), or upfield shifted (for all the other vanadium oxide structures) with increasing  $\text{V}_2\text{O}_5$  components, as presented in Table 2.

The refractive indices, conductivities, and densities of the  $x\text{V}_2\text{O}_5\text{-B}_2\text{O}_3\text{-yNa}_2\text{O}$  glasses were enhanced in a previous report but the glass transition temperature was lowered with increasing  $x$ .<sup>16</sup> In addition, the concentrations of both  $\text{V}^{4+}$  ions and total vanadium ions in a given volume were also raised, to which was attributed the enhanced conductivities at increasing  $x$ .<sup>16</sup> Our chemical shift data suggested that electron densities at each vanadium site were unevenly increased, even when both the weight densities and vanadium ion densities of the  $x\text{V}_2\text{O}_5\text{-B}_2\text{O}_3\text{-yNa}_2\text{O}$  glasses were enhanced.  $\text{V}^{4+}$  ions and vanadium oxide structures next to  $\text{V}^{4+}$  ions were not detected in the  $^{51}\text{V}$  MAS NMR spectra since the dipole interaction with the unpaired electrons of the  $\text{V}^{4+}$  ions makes the linewidth undetectably wide, especially when a superexchange interaction is present in the  $\text{V}^{4+}\text{-O-V}^{4+}$  chains.<sup>23,24</sup> Thus, the vanadium oxide structures with reduced populations at high  $\text{V}^{4+}$  ion concentrations, such as the  $\text{VO}_4$  structures with at least one oxygen bonded to boron and those bonded to neighboring vanadiums, were more likely to be the vanadium oxide structures right next to  $\text{V}^{4+}$  ions. However, this was not clearly elucidated in the absence of additional direct evidence to support it.

### Conclusions

The local structures of the boron and vanadium sites in the ternary glass system  $x\text{V}_2\text{O}_5\text{-B}_2\text{O}_3\text{-yNa}_2\text{O}$  were probed by  $^{11}\text{B}$  and  $^{51}\text{V}$  MAS NMR. The  $^{11}\text{B}$  MAS NMR results confirmed the production of more  $\text{BO}_3$  structures than  $\text{BO}_4$  structures with increasing  $x$ .  $\text{V}_2\text{O}_5$  and  $\text{Na}_2\text{O}$  were found to play opposite roles in terms of the local structures at the B sites. Our NMR

data suggested that  $\text{Na}_2\text{O}$  converted some of the  $\text{BO}_3$  structures into  $\text{BO}_4$  structures by donating oxygens, induced greater electric field gradients, but reduced the distortion of the electric field gradients at the boron sites of the  $\text{BO}_3$  structures. From the  $^{51}\text{V}$  spectra, the  $\text{VO}_4$ ,  $\text{VO}_5$  and  $\text{VO}_6$  structures with all oxygens bonded to the vanadium neighbors were identified, as were the  $\text{VO}_4$  structures, with at least one oxygen bonded to boron instead of vanadium, at low  $\text{Na}_2\text{O}$  content of  $y = 0.25$ . With increasing  $\text{Na}_2\text{O}$  content in the glass, the vanadium sites coordinated with greater number of oxygens were more populated while less V-O-B bonding was observed. The electron densities at different vanadium oxide structures did not change uniformly with variation in weight densities and vanadium ion densities. The  $\text{VO}_4$  structures were more likely to be vanadium oxide structures right next to  $\text{V}^{4+}$  ions. In future study on this glass system, we aim to clarify the local structure networks by heteronuclear correlation-type NMR experiments and to correlate the functionalities of the glasses with the structure networks.

**Acknowledgments.** This work was supported by the KBSI through research grants B2731B and B2831B.

### References

- Denton, E. P.; Rawson, H.; Stanworth, J. E. *Nature* **1954**, *173*, 1030.
- Baynton, P. L.; Rawson, H.; Stanworth, J. E. *J. Electrochem. Soc.* **1957**, *104*, 237.
- Ahmed, M. M.; Hogarth, C. A. *J. Mater. Sci.* **1983**, *18*, 3305.
- Culea, E.; Nicula, A. *Solid State Commun.* **1986**, *58(8)*, 545.
- Landsberger, F. R. *Ph.D. Thesis, Brown University*, 1970.
- Song, S. K.; Park, M. J. *New Phys.* **1989**, *29(5)*, 619.
- Balaji Rao, R.; Gopal, N. O.; Veeriah, N. *J. Alloys. Comp.* **2004**, *368*, 25.
- Zhong, J.; Bray, P. J. *J. Non-Cryst. Solids* **1989**, *111*, 67.
- Yun, Y. H.; Bray, P. J. *J. Non-Cryst. Solids* **1978**, *30*, 45.
- Jung, J. K.; Song, S. K.; Noh, T. H.; Han, O. H. *J. Non-Cryst. Solids* **2000**, *270*, 97.
- Hayakawa, S.; Yoko, T.; Sakka, S. *J. Non-Cryst. Solids* **1995**, *183*, 73.
- Sakida, S.; Hayakawa, S.; Yoko, T. *J. Phys.: Condens. Matter* **2000**, *12*, 2579.
- Shu, X.; Xuwen, W. *Chinese J. Magn. Reson.* **1990**, *7(3)*, 345.
- Gee, B. A.; Wong, A. *J. Phys. Chem. B* **2003**, *107*, 8382.
- Szalay, Z.; Rohonczy, J. *J. Non-Cryst. Solids* **2007**, *353*, 295.
- Kang, J. P. *Ph.D. thesis, Myoungji University*, 2006.
- Na, J. A.; Jeoung, M. H.; Kang, J. S.; Chung, H. J.; Kim, H. T.; Moon, S. J.; Kim, W. H.; Chung, S. J.; Kim, M. S. *J. Sci. Edu.* **1999**, *23*, 139.
- Skibsted, J.; Nielsen, N. Chr.; Bildsoe, H.; Jakobsen, H. J. *J. Am. Chem. Soc.* **1993**, *115*, 7351.
- Seshasayee, M.; Muruganandam, K. *Solid State Commun.* **1998**, *105*, 243.
- Shubin, A. A.; Lapina, O. B.; Courcot, D. *Catal. Today* **2000**, *56*, 379.
- Wei, D.; Wang, H.; Feng, X.; Chueh, W. T.; Ravikovitch, P.; Lyubovskiy, M.; Li, C.; Takeguchi, T.; Haller, G. L. *J. Phys. Chem. B* **1999**, *103*, 2113.
- Lapina, O. B.; Shubin, A. A.; Khabibulin, D. F.; Terskikh, V. V.; Bodart, P. R.; Amoureux, J. P. *Catal. Today* **2003**, *78*, 91.
- Khasa, S.; Seth, V. P.; Gupta, S. K.; Krishna, R. M. *Phys. Chem. Glasses* **1999**, *40(5)*, 269.
- Garbarczyk, J. E.; Wasiucionek, M.; Józwiak, P.; Tykarski, L.; Nowiński, J. L. *Solid State Ionics* **2002**, *154*, 367.